HKB PUBLICATIONS

ANALYTICAL CHEMISTRY LETTERS

Taylor & Francis
Taylor & Francis Group

DOI: 10.1080/22297928.2025.2564845

Research Article

Design, synthesis of substituted oxadiazol-2-yl-methanimine derivatives and evaluation for their anti-Alzheimer activity

R. Gandhimathi[2], M. Magesh[1]*, L. Kaviarasan[3], Madhuri Latha Thadanki [4], Vijaya Kishore Kanakaraju[5], D. Bharathi[6]

[1] Department of Pharmaceutical Chemistry, Saveetha College of Pharmacy, Saveetha Institute of Medical and Technical Sciences, Thandalam, Chennai 602105, Tamil Nadu, India
[2] Department of Pharmaceutical Chemistry and Analysis, School of Pharmaceutical Sciences, Vels Institute of Science, Technology and Advanced Studies (VISTAS), Pallavaram, Chennai-600117, Tamil Nadu, India
[3] Department of Pharmaceutical Chemistry, School of Pharmacy, Sathyabama Institute of Science and Technology, Chennai, India
[4] Department of Pharmaceutical Chemistry, College of Pharmaceutical Sciences, Acharya Nagarjuna University, Guntur, Andhra Pradesh, India
[5] Department of Pharmaceutics, NNRG school of pharmacy, Chowdariguda(V), Korremula X Roads, Ghatkesar (M), Medchel- Malkajigiri Dt, Hyderabad, India
[6] PSG College of Pharmacy, Department of Pharmaceutical Chemistry, Coimbatore, Tamil Nadu, India

***Corresponding Author**
M. Magesh
mageshjeevi2010@gmail.com

Received 12 My 2025
Revised 06 September 2025
Accepted 07 September 2025

Abstract
Alzheimer's disease is a progressive neurodegenerative disorder marked by cognitive decline, in which cholinergic dysfunction plays a central role. Current acetylcholinesterase (AChE) inhibitors such as donepezil provide only symptomatic relief and are limited by adverse effects and reduced long-term efficacy. To address these limitations, a series of N-(5-styryl-1,3,4-oxadiazol-2-yl)methanimine derivatives was designed by replacing the indanone moiety of donepezil with a 1,3,4-oxadiazole scaffold. The compounds were evaluated using in-silico drug-likeness prediction, ADMET profiling, and molecular docking against AChE (PDB ID: 4EY6). Molecular docking results revealed strong binding affinities, with docking scores ranging from -8.2 to -10.1 kcal/mol, comparable to that of donepezil and followed by synthesis and structural confirmation through IR, NMR, and mass spectrometry. The most potent cholinesterase catalytic domain inhibition was observed in compound 2 (IC_{50} = 25.71±0.26 µM), which is nearly equivalent to the reference standard, donepezil (IC_{50} = 24.71 µM). The inhibitory action of compound 2 was superior to that of the other examined compounds. All synthesized compounds were screened for *in vitro* cytotoxicity against human SH-SY5Y neuroblastoma cell lines. The viability of cells at the maximum concentration of compound 2 was found to be 91.29%, which is comparable to the standard (93.35%). The remaining compounds exhibited moderate to good neuroprotective activity, with concentration-dependent neuroprotective effects observed in all compounds, except for a few. These findings suggest that oxadiazolyl methanimine derivatives represent promising scaffolds for further development as potential anti-Alzheimer's agents.

Keywords
Anti-cholinesterase, oxadiazole, docking, Donepezil, SH-SY5Y, ADME.

Introduction

The disease was first described in 1907 by German scientist Alois Alzheimer, who characterized it as a progressive degeneration of the nervous system[1]. As the disease advances, cognitive functions steadily decline, accompanied by severe behavioral abnormalities such as restlessness, irritability, disorientation, depression, and anxiety[2]. Modern definitions emphasize its nature as a neurodegenerative disorder with irreversible effects. Symptoms include memory loss, confusion, impaired intellect, social withdrawal, and poor judgment, resulting from the loss of neurons in the cerebral cortex and hippocampus[3-5]. Alzheimer's disease (AD) is the most common type of dementia, and it is projected that 152 million people will be affected by 2050 unless effective preventive measures or cures are developed[6]. The prevalence of AD is typically 2-3% among individuals aged 70-75 years, rising to 20-25% in those aged 85 and older. It remains unclear whether the incidence of AD is still rising or stabilizing. Women are at a higher risk of developing Alzheimer's compared to

men, largely due to age-adjusted differences in risk. Research has also suggested that the prevalence of AD varies across countries and is influenced by social and economic factors. Acetylcholinesterase (AChE) and butyrylcholinesterase (BuChE) are the two most prominent cholinesterase enzymes in the central nervous system. These enzymes, which belong to the carboxylesterase family, are responsible for the hydrolysis of acetylcholine (ACh) during cholinergic transmission. In healthy individuals, AChE hydrolyzes approximately 80% of ACh, while BuChE has a less significant role. However, studies show that, as Alzheimer's disease progresses, BuChE activity increases by 40-90%, while AChE activity decreases by 75-80%, particularly in the hippocampus and temporal cortex[7].

A major limitation of current treatments for Alzheimer's is the presence of central and peripheral side effects in drugs designed to slow disease progression[8,9]. This has created a growing demand for more effective and safer acetylcholinesterase inhibitors. Donepezil, a selective AChE inhibitor with minimal effect on BuChE, is commonly prescribed for AD due to its longer half-life and fewer adverse effects[10]. However, while donepezil can help alleviate symptoms, it is not effective in treating moderate to severe stages of the disease[11]. In light of this, we have focused on developing more potent inhibitors of AChE, starting with donepezil, to potentially offer better outcomes in advanced stages of the disease[12].

Heterocyclic compounds, which contain at least one element other than carbon (such as nitrogen, sulfur, or oxygen), are an important class of organic compounds. Oxadiazoles, a frequent structural feature in drug-like compounds, are often used as bioisosteric replacements for amides and esters. Recent literature highlights the diverse biological activities of 1,3,4-oxadiazoles and their derivatives, including antimicrobial[13], tuberculostatic[14], anti-inflammatory[15], antifungal[16], antibacterial[17], anticancer[18], analgesic[19], anticonvulsant[20], anti-hepatitis B, and antiparasitic[21] properties. Several oxadiazole-containing drugs are in late-stage clinical trials, such as the antiviral drug raltegravir[23], the anticancer agent zibotentan[22], and the cystic fibrosis treatment ataluren. Additionally, several other drugs containing 1,3,4-oxadiazole units are currently used therapeutically, including ABT-751 (antibiotic)[27], Furamizole (antibiotic)[28], MK-0633 p-toluenesulfonate (5-lipoxygenase inhibitor)[25], Nesapidil (antihypertensive)[26], and Fenadiazole (hypnotic)[24]. The synthesis of 1,3,4-oxadiazoles is well-documented in the literature, and **Figure 1** illustrates medications containing oxadiazole derivatives.

The design of the synthesized hybrids was rationalized by combining the pharmacophoric features of donepezil with the bioactive 1,3,4-oxadiazole scaffold. Donepezil, a clinically established AChE inhibitor, contains an indanone moiety crucial for interactions within the catalytic and peripheral anionic sites of AChE, but its clinical utility is limited by side effects and declining efficacy over long-term use. Literature reports highlight 1,3,4-oxadiazoles as versatile pharmacophores with neuroprotective, antioxidant, and potent cholinesterase inhibitory

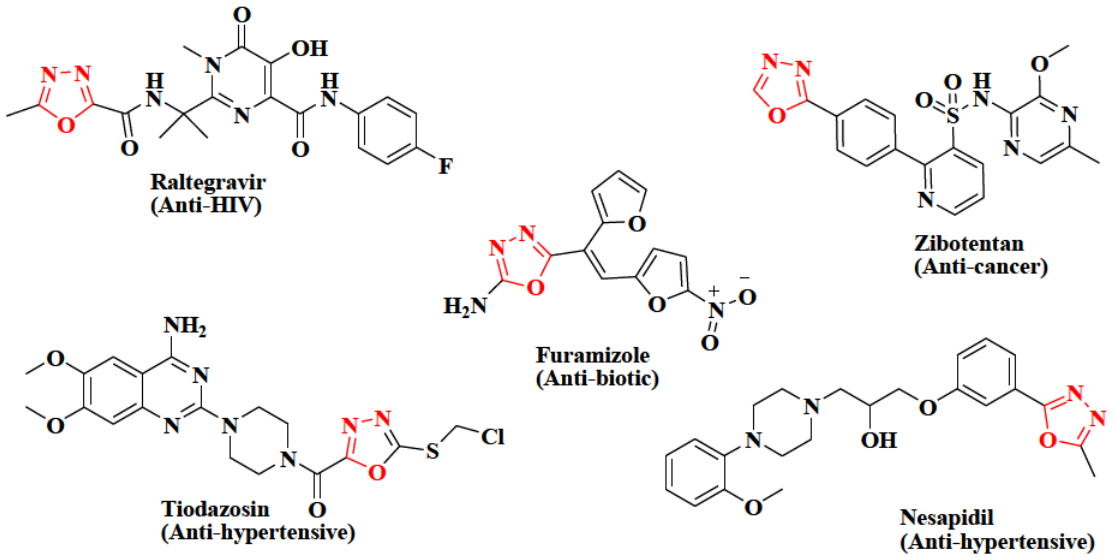

Figure 1. List of oxadiazole-containing drugs

activities. Importantly, the 1,3,4-oxadiazole ring serves as a bioisosteric replacement for carbonyl-containing groups such as indanones, offering improved metabolic stability, favorable hydrogen-bonding interactions, and enhanced blood-brain barrier penetration. Incorporation of this scaffold into the donepezil framework was therefore expected to retain essential AChE-binding interactions while improving drug-likeness and pharmacokinetic properties. Moreover, such hybridization has the potential to generate dual-site inhibitors capable of targeting both the catalytic active site and the peripheral anionic site of AChE, thereby enhancing potency and potentially mitigating amyloid-β aggregation associated with Alzheimer's pathology[25-27]. This study details the synthesis, biological evaluation, docking analysis, and ADME prediction of the compounds.

Materials and methods

All reagents and solvents used were of analytical reagent grade and were subjected to appropriate drying and purification procedures. Reactions were performed in glassware that had been oven-dried unless stated otherwise. Reagents and solvents were either directly purchased or purified by recrystallization or redistillation. The purity of the synthesized compounds was verified using thin-layer chromatography (TLC). TLC was conducted on silica gel 60 F254 plates (Merck), with aluminum as the support material, with a plate thickness of 0.25 mm. A mobile phase of n-hexane:ethyl acetate (1:1) was used to monitor the reaction progress. Iodine vapor was employed for visualization of the chromatograms. Melting points were determined using open capillary tubes and recorded without correction on a Veego VMP-1 melting point apparatus. Infrared (IR) spectra were obtained using a Perkin-Elmer Fourier Transform Infrared (FT-IR) Spectrometer with KBr pellets. Proton (^{1}H) and carbon-13 (^{13}C) nuclear magnetic resonance (NMR) spectra were recorded at 400 MHz on a Bruker NMR Spectrometer (Billerica, MA, USA), with tetramethylsilane (TMS) as the internal standard for chemical shift measurements in ppm. Mass spectra of selected compounds were recorded using a Shimadzu LC-MS/MS instrument.

In silico evaluation of oxadiazolyl methanimine libraries

The oxadiazole nucleus was explored by modifying the substituents at the C2 and C5 positions. This led to the creation of 100 novel structures using computational tools such as ChemSketch and ChemDraw, as shown in Supplementary Figure **SX1**. These designed molecules were then subjected to *in-silico* evaluations, including the prediction of pharmacokinetic properties, drug-likeness characteristics, and their potential to bind with target proteins. *In-silico* evaluation is an essential step in determining whether a molecule will be effective before its synthesis. Literature evidence supports the fact that compounds designed through *in-silico* studies often succeed in various aspects. The advantage of *in-silico* evaluation lies in its predictive approach, which helps researchers design novel compounds for safe and effective medication. This contrasts with traditional methods that involve the random synthesis of molecules. The rational approach provided by *in-silico* evaluation assists medicinal chemists in developing compounds with broad pharmacological activities while ensuring safety and effectiveness.

Drug likeness studies

Molinspiration forecasting was used in a computer simulation to forecast the drug likeness properties of proposed substances. The aforementioned parameters are computed here. Infractions of the rule-of-three, rule-of-five, and drug likeness were determined. A molecule can only be given orally if it meets the following requirements[28].

- Molecular weight (MW) - Less than 500 daltons
- Number of H - bond donors - Less than 5
- Number of H - bond acceptors - Less than 10
- Polar surface area (PSA) - Less than 60 A^{o}
- Log P (n- octanol -water partition co-efficient)che, - Less than 5

ADME prediction

The Swiss ADME tool was utilized in a computer simulation to predict the pharmacokinetic properties of proposed compounds, including their potential for oral absorption in humans and ability to cross the blood-brain barrier (BBB). The attributes provided help in understanding the ADME characteristics of the compounds.

Molecular docking studies

In contemporary drug development, molecular docking plays a crucial role in understanding the interaction between enzymes or receptors and small organic molecules. It is commonly used to identify the specific interactions between target proteins and

potential drug candidates. For *in-silico* research, various computational biology tools are employed. The protein structure used in this study was obtained from the Protein Data Bank (www.rcsb.org/pdb). Molecular docking simulations were then performed using the offline platform PyRx V0.9[29].

Preparation of protein

The acetylcholinesterase (PDB:4EY6) with a resolution of 1.90A° using the offline programme Protein Data Bank. Eliminate the crystal water from the proteins before adding the missing hydrogens, protonation, ionization, and energy minimization.

Preparation of ligands

The Chemdraw ultra tool is used to build the molecules as 2D and 3D structures. After the molecule was created, Marvin Sketch was used to 3D optimize the structure, which was then saved as SDF.

Molecular docking

- Ligands (SDF) were imported in to the PyrX
- Energy of the imported ligands were minimized
- Ligands (SDF) were converted into PDBQT format
- Loaded the protein as macromolecule
- Protein (PDB) was converted into PDBQT format
- Grid box were defined
- Autodock vina has chosen has docking algorithm
- Multiple docked poses of the ligands to an active site pocket of protein generated in the PyrX platform and the binding affinity of the different poses of each ligands towards target protein was also calculated.

Analysis and visualization of the results

The binding energies and RMSD values of various ligand poses were analyzed to determine the most favorable interaction with the protein. The interactions between the ligands and the protein were visualized using Discovery Studio Visualizer, allowing for both 2D and 3D representations.

Chemistry

Synthesis of 5-styryl-1,3,4-oxadiazol-2-amine (A)

Semicarbazide (50 mmol) and cinnamic acid (50 mmol) were combined with sulfuric acid (13 mL) in a round-bottom flask and heated for 35 to 45 minutes at a temperature range of 65 to 75°C. After heating, the mixture was allowed to cool to room temperature (approximately 1 hour) in an ice bath. Following this, 100 mL of distilled water was added dropwise at first, then slowly in 5-7 mL increments as the fuming subsided. A reflux condenser was then set up, and the reaction mixture was heated for an additional 22-24 hours. The reaction progress was monitored using TLC, with n-hexane: ethyl acetate (7:3) as the mobile phase. After the reaction was complete, 50% sodium hydroxide was added, and the mixture was stirred continuously and allowed to cool. The resulting mixture was basified, and the solids were filtered and washed with distilled water. The product was air-dried and purified by recrystallization from ethanol.

General procedure for synthesis of N-(5-styryl-1,3,4-oxadiazol-2-yl)methanimine derivatives (1-5 and 51 - 55)

The reaction mixture was prepared by adding 5-phenyl-1,3,4-oxadiazol-2-amine (0.01 mol) to 10-12 mL of 100% ethyl alcohol in a 25 mL round-bottom flask, with NaOH pellets. This mixture was then used to reflux the corresponding aromatic and heteroaromatic aldehydes (0.01 mmol). The reaction progress was monitored by TLC using a mobile phase of n-hexane: ethyl acetate (7:3). Once the reaction was complete, the contents were poured into a Petri dish and the solvent was allowed to evaporate by air. To remove any excess base, the product was washed with diluted HCl for neutralization.

1-(4-Fluorophenyl)-N-(5-((E)-styryl)-1,3,4-oxadiazol-2-yl) methanimine (1)

The reaction mixture was then treated with 4-fluorobenzaldehyde and processed following the standard procedure for synthesizing N-(5-styryl-1,3,4-oxadiazol-2-yl)methanimine derivatives. The resulting solid was filtered, dried, and washed with a dilute hydrochloric acid solution. Recrystallization was carried out using ethanol. IR V_{max} cm^{-1}(KBr): 2985 (CH stretching alkene), 2600(CH stretching aromatic), 1372 (CN bending) 851 (Aromatic ring) and 759 (C-Halogen stretching). ^{1}H NMR (DMSO ppm) (400 MHz) δ: 9.82 (s, 1H, aromatic proton), 8.33 (s, 2H, aromatic proton), 7.46 (s, 1H, aromatic proton), 7.41 (d, J = 1.9 Hz, 2H, aromatic proton), 7.36 (m, 2H, aromatic proton), 7.28 (m, 2H, CH proton alkene), 7.15 (m, 1H, CH proton alkene); ^{13}C NMR (DMSO ppm) (101 MHz) δ: 168.73 (C-O carbon), 168.20 (C-O carbon), 149.11 (C-N carbon), 148.29 (C-F carbon), 147.70, 146.58, 145.76, 144.04, 143.46 (aromatic carbons), 142.33 (C=C carbon),

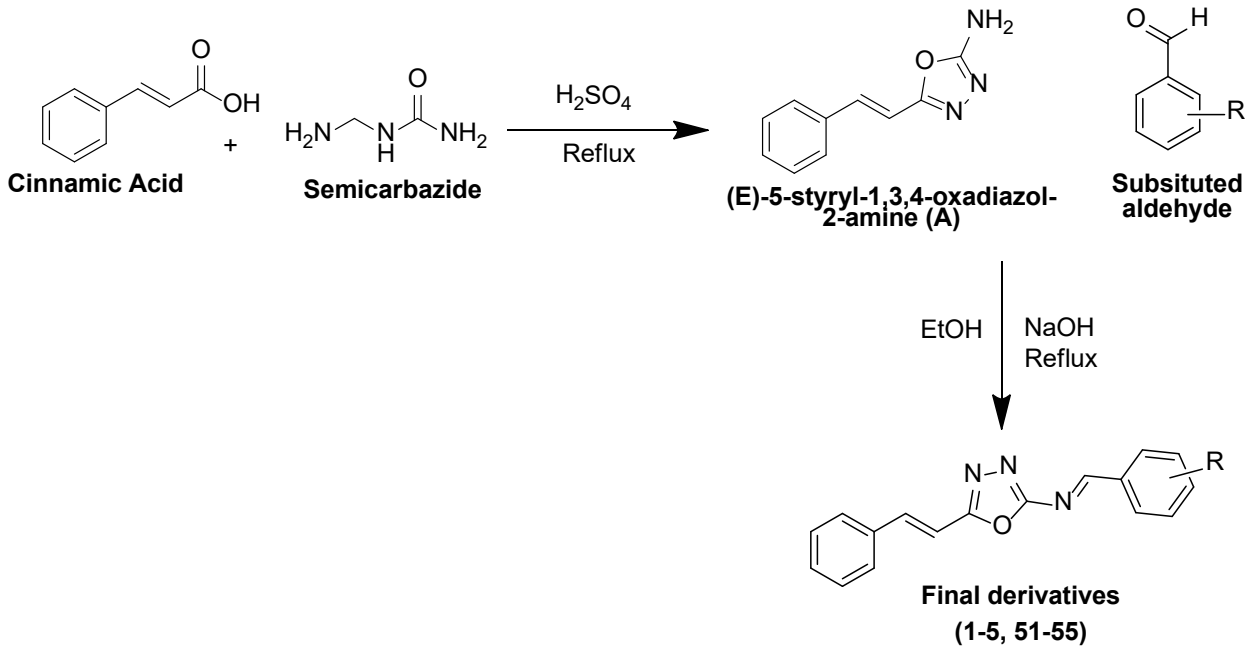

Scheme 1. General procedure for synthesis of final derivatives

141.22 (C=C carbon); Mass m/z: [M+23] peak was observed at 315 m/z.

1-(Pyridin-4-yl)-N-(5-((E)-styryl)-1,3,4-oxadiazol-2-yl)methanimine (2)

The reaction mixture, as described in the general procedure, was treated with pyridine-4-carbaldehyde. Following the standard procedure for the synthesis of N-(5-styryl-1,3,4-oxadiazol-2-yl)methanimine derivatives, the resulting solid was filtered, dried, and washed with a dilute hydrochloric acid solution. Recrystallization was performed using ethanol. IR V_{max} cm^{-1}(KBr): 1372 (CN bending) 851 (Aromatic ring) and 759; ^{1}H NMR (DMSO ppm) (400 MHz) δ: 10.13 (m, 1H, aromatic proton), 8.66 (s, 1H, aromatic proton), 7.94 (s, 2H, aromatic proton), 7.87 (s, 2H, aromatic proton), 7.80 (s, 2H, aromatic proton), 7.71 (s, 1H, aromatic proton), 7.65 (s, 2H, aromatic proton), 6.71 (m, 2H, CH proton alkene), 6.60 (m, 1H, CH proton alkene); ^{13}C NMR (DMSO ppm) (101 MHz) δ: 155.82 (C-O carbon), 154.37 (C-O carbon), 134.50 (C-N carbon), 130.00, 129.31, 128.03, 127.26, 127.03, 124.46 (Aromatic carbon), 119.01 (C=C carbon); Mass m/z: [M+1] peak was observed at 277 m/z.

1-Phenyl-N-(5-((E)-styryl)-1,3,4-oxadiazol-2-yl) methanimine (3)

The reaction mixture was treated with benzaldehyde, and the procedure for synthesizing N-(5-styryl-1,3,4-oxadiazol-2-yl)methanimine derivatives was followed. The resulting solid was filtered, washed with a dilute hydrochloric acid solution, and then dried. Recrystallization was performed using ethanol. IR V_{max} cm^{-1}(KBr): 2985 (CH stretching alkene), 1372 (CN bending), 851 (Aromatic ring); ^{1}H NMR (DMSO ppm) (400 MHz) δ: 9.49 (m, 1H, aromatic proton), 7.69 (m, 1H, aromatic proton), 7.47(m, 1H, aromatic proton), 7.33 (m, 2H, aromatic proton), 7.16 (d, J = 1.9 Hz, 2H, aromatic proton), 7.06 (m, 2H, aromatic proton), 6.98 (s, 2H, CH proton alkene), 6.94 (s, 1H, CH proton alkene); ^{13}C NMR (DMSO ppm) (101 MHz) δ: 155.82 (C-O carbon), 134.50 (C-O carbon), 132.33 (C-N carbon), 131.21, 130.00, 129.31, 128.03, 127.26, 127.03 (Aromatic carbons), 124.46 (C=C carbons); Mass m/z: 275m/z.

1-(4-Chlorophenyl)-N-(5-((E)-styryl)-1,3,4-oxadiazol-2-yl) methanimine (4)

The reaction mixture described in the general procedure was treated with 4-chlorobenzaldehyde, and the synthesis of N-(5-styryl-1,3,4-oxadiazol-2-yl) methanimine derivatives was carried out following the outlined procedure. The resulting solid product was filtered, dried, and washed with a dilute solution of hydrochloric acid. Recrystallization was performed using ethanol. IR V_{max} cm^{-1}(KBr): 2985 (CH stretching alkene), 1372 (CN bending), 851(Aromatic ring). ^{1}H NMR (DMSO ppm) (400 MHz) δ: 9.49 (m, 1H, aromatic proton), 7.69 (m, 1H, aromatic proton), 7.47(m, 1H, aromatic proton), 7.33 (m, 2H, aromatic

proton), 7.16 (d,J=1.9 Hz, 2H, aromatic proton), 7.06 (m,2H, aromatic proton), 6.98 (s, 2H, CH proton alkene), 6.94 (s, 1H, CH proton alkene); ^{13}C NMR (DMSO ppm) (101 MHz) δ: 155.82 (C-O carbon), 134.50 (C-O carbon), 132.33 (C-N carbon), 131.21, 130.00, 129.31, 128.03, 127.26, 127.03 (Aromatic carbons), 124.46 (C=C carbons); Mass m/z: 309m/z.

2-(-({5-((E)-Styryl)-1,3,4-oxadiazol-2-yl}imino) methyl)phenol (5)

The reaction mixture was then treated with 2-hydroxybenzaldehyde and the procedure for synthesizing N-(5-styryl-1,3,4-oxadiazol-2-yl) methanimine derivatives was followed. The resulting solid was filtered, dried, and washed with a dilute hydrochloric acid solution. Recrystallization was performed using ethanol. IR V_{max} cm^{-1}(KBr): 2985 (CH stretching alkene), 2600 (CH stretching aromatic), 1374 (CN bending) 888 (Aromatic ring). ^{1}H NMR (DMSO ppm) (400 MHz) δ: 9.67 (m, 1H, aromatic proton), 7.46 (s, 1H, aromatic proton), 7.44 (m, 1H, aromatic proton), 7.41 (s, 2H, aromatic proton), 7.36 (s, 1H, aromatic proton), 7.24 (s, 1H, aromatic proton), 7.12 (d, J = 23.1 Hz, 1H, CH proton alkene), 7.08 (s, 1H, CH proton alkene); ^{13}C NMR (DMSO ppm) (101 MHz) δ: 156.63 (C-O carbon), 148.92 (C-O carbon), 148.39 (C-N carbon), 126.37, 125.64, 124.66, 124.43, 123.54, 123.24, 122.42, 121.82, 121.60, 120.70 (Aromatic carbon), 120.10 (C=C carbon); Mass m/z: [M-1] peak was observed at 290 m/z.

4-Bromo-2-((E)-((5-((E)-styryl)-1,3,4-oxadiazol-2-yl)imino)methyl)phenol (51)

The reaction mixture was treated with 2-methyl-3-bromobenzaldehyde, and the standard procedure for synthesizing N-(5-styryl-1,3,4-oxadiazol-2-yl) methanimine derivatives was followed. The resulting solid was filtered, dried, and washed with a dilute hydrochloric acid solution. Recrystallization was carried out using ethanol. IR V_{max} cm^{-1}(KBr): 2985 (CH stretching alkene), 2479 (CH stretching aromatic), 1374 (CN bending) 851 (Aromatic ring) and 761 (C-Halogen stretching); ^{1}H NMR (DMSO ppm) (400 MHz) δ: 9.84 (m, 1H, aromatic proton), 7.46 (s, 2H, aromatic proton), 7.44 (m, 2H, aromatic proton), 7.41 (s, 2H, aromatic proton), 7.36 - 7.24 (s, 1H, aromatic proton), 7.22 (s, J = 23.1 Hz, 1H, CH proton alkene), 7.12 (m, 2H, CH proton alkene); ^{13}C NMR (DMSO ppm) (101 MHz) δ: The 155.81 (C-O carbon), 154.84 (C-O carbon), 154.37 (C-N carbon), 134.50 (C-Br carbon), 130.10, 130.00, 129.31, 128.37, 128.03, 127.78, 127.26, 127.03 (Aromatic carbons), 124.45 (C=C carbon); Mass m/z: 269 m/z.

1-(4-Methoxyphenyl)-N-(5-((E)-styryl)-1,3,4-oxadiazol-2-yl)methanimine (52)

The reaction mixture was treated with 4-methoxybenzaldehyde, and the standard procedure for synthesizing N-(5-styryl-1,3,4-oxadiazol-2-yl) methanimine derivatives was followed. The resulting solid was filtered, dried, and washed with a dilute hydrochloric acid solution. Recrystallization was performed using ethanol. IR V_{max} cm^{-1} (KBr): 3203 (CH stretching alkene), 1557 (co stretching), 1099 (Aromatic ring) and 1380 (CN bending); ^{1}H NMR (DMSO ppm) (400 MHz) δ: 10.13 (m, 1H, aromatic proton), 7.87 (s, 2H, aromatic proton), 7.80 (m, 2H, aromatic proton), 7.48 (s, 2H, aromatic proton), 7.39 (s, 1H, aromatic proton), 7.24 (s, J = 23.1 Hz, 1H, CH proton alkene), 7.20 (m, 2H, CH proton alkene); ^{13}C NMR (DMSO ppm) (101 MHz) δ: 155.81 (C-O carbon), 154.37 (C-O carbon), 134.50 (C-N carbon), 130.00, 129.31, 128.03, 127.26, 127.03, 124.45 (Aromatic carbon), 119.01 (C=C carbon), 64.86 (methoxy carbon); Mass m/z: [M+1] peak was observed at 306 m/z.

(E)-1-(4-(Pyrrolidin-1-yl)phenyl)-N-(5-((E)-styryl)-1,3,4-oxadiazol-2-yl) methanimine (53)

The reaction mixture was then treated with 4-pyrrolidinyl benzaldehyde and the general procedure for synthesizing N-(5-styryl-1,3,4-oxadiazol-2-yl) methanimine derivatives was followed. After the reaction, the resulting solid was filtered, washed with a dilute hydrochloric acid solution, and dried. Recrystallization was carried out using ethanol. IR V_{max} cm^{-1}(KBr): 2985 (CH stretching alkene), 1380 (CN bending) (Aromatic ring); ^{1}H NMR (DMSO ppm) (400 MHz) δ: 9.74 (s, 1H, aromatic proton), 7.73 (m, 2H, aromatic proton), 7.47 (m, 2H, aromatic proton), 7.39 (s, 1H, aromatic proton), 7.26 (s, 22H, aromatic proton), 7.18 (s, 1H, aromatic proton), 7.01 (s, 2H, aromatic proton), 6.72 (m, 1H, CH proton alkene), 5.41 (s, 2H, CH proton alkene), 3.09 (d, J = 7.8 Hz, 2H, methoxy proton); ^{13}C NMR (DMSO ppm) (101 MHz) δ: 155.81 (C-O carbon), 154.37 (C-O carbon), 134.50 (C-N carbon), 129.99, 129.31, 128.03, 127.26, 127.03, 124.45 (Aromatic carbon), 119.01 (C=C carbon), 64.86 (CH carbons), 28.00 (CH carbons); Mass m/z: 344m/z.

2-(-({5-((E)-Styryl)-1,3,4-oxadiazol-2-yl}imino) methyl)benzenethiol (54)

The reaction mixture was then treated with 2-sulphanyl benzaldehyde, and the procedure for synthesizing N-(5-styryl-1,3,4-oxadiazol-2-yl)methanimine derivatives was followed. The resulting solid was filtered, dried, and washed with a dilute hydrochloric acid solution. Recrystallization was carried out using ethanol. IR V_{max} cm^{-1}(KBr): 2927 (CH stretching alkene), 2626 (CH stretching aromatic), 1391 (CN bending) and 849 (Aromatic ring); ^{1}H NMR (DMSO ppm) (400 MHz) δ: 10.16 (s, 1H, SH proton), 8.35 (dd, J = 16.3, 7.1 Hz, 2H, aromatic proton), 8.05 (m, 2H, aromatic proton), 7.64 (m, 1H, aromatic proton), 7.50 (t, J = 7.5 Hz, 1H), aromatic proton, 7.44 (s, 2H, aromatic proton), 7.32 (s, 1H, aromatic proton), 7.16 (s, 1H, aromatic proton), 6.93 (m, 1H, CH proton alkene), 6.79 (m, 2H, CH proton alkene); ^{13}C NMR (DMSO ppm) (101 MHz) δ: 155.67 (C-O carbon), 134.35 (C-O carbon), 133.75 (C-N carbon), 130.45, 129.81, 129.20, 127.64, 127.00, 126.66, 124.30 (Aromatic carbon), 118.38 (C=C carbon); Mass m/z: 307 m/z.

1-(5-Methoxypyridin-3-yl)-N-(5-((E)-styryl)-1,3,4-oxadiazol-2-yl)methanimine (55)

The reaction mixture was treated with 5-methoxypyridine-3-carbaldehyde, and the synthesis of N-(5-styryl-1,3,4-oxadiazol-2-yl)methanimine derivatives was carried out following the general procedure. The resulting solid was filtered, washed with dilute hydrochloric acid solution, and then dried. Recrystallization was performed using ethanol. IR V_{max} cm^{-1}(KBr): 2930 (CH stretching alkene), 2646 (CH stretching aromatic), 1434 (CN bending), 896 (Aromatic ring) and 759 (C-Halogen stretching); ^{1}H NMR (DMSO ppm) (400 MHz) δ: 9.88 (s, 1H, aromatic proton), 7.69 (d, J = 25.7 Hz, 2H, aromatic proton), 7.63 (s, 1H, aromatic proton), 7.49 (s, 2H, aromatic proton), 7.21(s, 1H, aromatic proton), 7.12 (s, 1H, CH proton alkene), 7.00 (s, 2H, CH proton alkene), 3.31 (m, 3H, methoxy proton); ^{13}C NMR (DMSO ppm) (101 MHz) δ: The ^{13}C NMR spectra of compound 155 showed peaks at 155.82 (C-O carbon), 154.37 (C-O carbon), 130.00 (C-N carbon), 129.31, 128.98, 128.03, 127.26, 127.03, 126.66, 125.85, 124.46 (C=C carbon), 64.86 (methoxy carbon); Mass m/z: 306 m/z.

In vitro evaluation of neuroprotective activity of synthesized compounds by MTT assay method

The MTT assay is a colorimetric technique used to measure the metabolic activity of cells. NAD(P)H-dependent cellular oxidoreductase enzymes can, in some cases, indicate the number of viable cells in a sample. The tetrazolium dye 3-(4,5-dimethylthiazol-2-yl)-2,5-diphenyltetrazolium bromide (MTT) can be chemically reduced by these enzymes to form an insoluble purple formazan. The number of viable cells is closely correlated with the intensity of the purple color, which can be used to calculate the percentage of cell viability[30].

Cell culture

Sigma-Aldrich supplied a set of human SH-SY5Y neuroblastoma cells, which were cultured in Dulbecco's Modified Eagle Medium (DMEM) supplemented with 10% fetal bovine serum (FBS) at 37°C in a humidified environment with 5.0% CO_2. Investigations were conducted when the cells reached 80% confluence.

Procedure

The MTT (3-(4,5-dimethylthiazol-2-yl)-2,5-diphenyl-tetrazolium bromide) colorimetric assay is commonly used to measure metabolic activity and cell viability. In the context of neuroprotection from beta-amyloid (Aβ) damage, the basic procedure of the MTT assay involves the following steps: Cell viability was determined using the standard MTT reduction test with triplicate measurements for each concentration. Briefly, 100 µL of fresh medium supplemented with 10% fetal bovine serum (FBS) was added to each well of a 96-well plate. Cells were seeded at a density of 2.0 x 10^4 per well. After a 24-hour stabilization period, the cells were pretreated for 2 hours with five different concentrations of the test drug (5, 10, 20, 40, and 80 µM, dissolved in DMEM with 10% FBS). Following this, the drug treatment was mixed with 10 µM Aβ 25-35 and incubated for an additional 24 hours at 37°C in a 5% CO_2 atmosphere. For statistical analysis, a solvent control condition consisting of DMEM and 10% FBS was used. After the treatment period, the culture media was removed, and 100 µL of MTT (500 µg/mL) was added to each well. The plates were then incubated for 4 hours. To dissolve the dark blue formazan crystals, 100 µL of DMSO was added to each well after removing the MTT solution. The plates were gently shaken and then read with a microplate reader at 540 nm. Data analysis was performed by calculating the percentage of cell viability relative to the control group.

In vitro evaluation of acetylcholinesterase inhibitory activity

The acetylcholinesterase inhibitory activity of the synthesized compounds was assessed using the colorimetric method developed by Ellman et al., with slight modifications. This method is based on the enzymatic hydrolysis of acetylthiocholine iodide (ATCI) by AChE, which produces thiocholine. Thiocholine subsequently reacts with 5,5'-dithiobis-(2-nitrobenzoic acid) (DTNB, also known as Ellman's reagent) to form a yellow-colored 5-thio-2-nitrobenzoate anion. The intensity of this yellow color, measured at 412 nm using a microplate reader, is directly proportional to the enzyme's activity. In the presence of an inhibitor, the color intensity decreases, indicating inhibition of AChE.

The assay was carried out in a 96-well microplate format. Acetylcholinesterase (Type VI-S from Electrophorus electricus), ATCI, and DTNB were obtained from Sigma-Aldrich, and Tris-HCl buffer (50 mM, pH 8.0) was used as the assay medium. The synthesized test compounds were dissolved in DMSO and diluted to appropriate concentrations (1, 10, 50, and 100 µM) using the buffer. The final concentration of DMSO in all wells was kept below 1% to avoid solvent-induced interference with enzyme activity.

To each well of the microplate, 140µL of Tris-HCl buffer, 20 µL of test compound or standard (donepezil), and 20 µL of the AChE enzyme solution (0.5 U/mL) were added. The plate was incubated at 37°C for 15 minutes to allow pre-incubation of the enzyme with the inhibitors. Following this, 10µL of DTNB (0.3 mM) and 10 µL of ATCI (0.71 mM) were added to initiate the reaction, making the total volume in each well 200 µL. The mixture was gently shaken and further incubated at 37°C for 30 minutes. After incubation, the absorbance was measured at 410 nm using a microplate reader[31]. All measurements were performed in triplicate. The percentage of enzyme inhibition was calculated using the formula:

$$\% \text{ Inhibition} = \left(1 - \frac{A_{sample}}{A_{control}}\right) \times 100$$

Results and discussions

ADMET prediction

In this study, a total of 100 molecules were designed based on literature reports of oxadiazole derivatives. These compounds underwent *in silico* evaluation to predict their behavior. Drug-likeness and pharmacokinetic parameters were determined using www.SwissADME.org. It is important to note that these tools provided valuable insights; however, the predictions made by Swiss ADME were considered as preliminary studies and computational models for drug design and optimization. For AD, it is essential that drugs effectively penetrate the BBB to reach their target sites in the brain, where they can exert their therapeutic effects. If a drug cannot efficiently penetrate the BBB, it may fail to reach its intended target, limiting its effectiveness as a treatment for AD. The physicochemical characteristics of the oxadiazolyl methanimine derivatives are provided in **Table 1**. Oxadiazole hybrids are known for their excellent ability to penetrate the BBB compared to other heterocyclic compounds. Therefore, the oxadiazole moiety was selected to evaluate the anti-Alzheimer activity. Not surprisingly, almost all the designed oxadiazole derivatives demonstrated potential BBB penetration when subjected to *in-silico* evaluation via Swiss ADME. Molecules containing polar substituents tend to have a reduced capacity to traverse the BBB. In this study, the non-polar nature of the molecules was further enhanced by the addition of cinnamic acid, which provided sufficient non-polarity to the synthesized compounds. Studies have shown that the topological polar surface area (TPSA) of an organic compound is inversely related to its BBB penetration capacity. To optimize BBB penetration, we designed compounds with fewer polar substituents and sufficiently long alkyl side chains to maintain the TPSA within an acceptable range. Oxadiazoles have shown moderate to good inhibitory potential against acetylcholinesterase, and substitution patterns also influence the enzyme inhibitory activity. Some studies suggest that halogenated oxadiazoles exhibit promising inhibitory activity against cholinesterases. Furthermore, heteroatoms within the aromatic ring can alter the molecule's electronic distribution, potentially improving its interaction with biological targets. This electronic manipulation may further enhance the compound's pharmacological action.

Molecular docking studies

Cholinesterases are crucial enzymes in the development of Alzheimer's disease (AD). Molecules intended as anti-AD agents should effectively inhibit these enzymes to maintain acetylcholine levels, a vital substance required for cognitive functions such as rational thinking and memory. Therefore,

Table 1. Physico-chemical characteristics of oxadiazolyl methanimine derivatives

S. No	Compound No.	Mol. formula	Mol. weight	No. of atoms	No. of rotatable bonds	No. of H bond donors	No. of H bond acceptors	TPSA	Log P	GI absorption	BBB penetration	Violations of drug likeness rules	AMES Toxicity	Hepato toxicity
1	1	$C_{17}H_{12}FN_3O$	293	34	4	0	5	51.28	3.41	High	Yes	0	No	No
2	2	$C_{16}H_{12}N_4O$	276	33	4	0	5	64.17	2.82	High	Yes	0	No	No
3	3	$C_{19}H_{19}N_3O$	305	42	4	0	4	51.28	4.66	High	Yes	0	No	No
4	4	$C_{19}H_{18}ClN_3O$	339	42	4	0	4	51.28	5.04	High	Yes	0	No	No
5	5	$C_{19}H_{19}N_3O_2$	321	43	4	1	5	71.51	4.75	High	Yes	0	No	No
6	51	$C_{17}H_{12}BrN_3O_2$	370	35	4	1	5	71.51	3.11	High	Yes	0	No	No
7	52	$C_{18}H_{15}N_3O_2$	305	38	5	0	5	60.51	3.55	High	Yes	0	No	No
8	53	$C_{21}H_{20}N_4O$	344	46	5	0	4	54.52	3.82	High	Yes	0	No	No
9	54	$C_{17}H_{13}N_3OS$	307	35	4	0	4	90.08	3.42	High	No	0	No	No
10	55	$C_{17}H_{14}N_4O_2$	306	37	5	0	6	73.4	3.3	High	Yes	0	No	No

inhibiting these enzymes is beneficial for alleviating the symptoms of AD patients. Acetylcholinesterase (PDB ID: 4EY6) is considered a target protein for molecular docking studies. In this study, 100 molecules were designed based on literature studies of oxadiazole derivatives, and these compounds underwent molecular docking experiments. The PyRx 0.9 software was used to predict how the protein would interact with its inhibitors. To assess the binding capabilities of cholinesterase and the 100 oxadiazole analogues, molecular docking was performed. The standard compounds, donepezil, along with the synthesized compounds, were docked with cholinesterase. The docking energies of the designed compounds ranged from 7 to 11 kcal/mol, indicating good binding affinities to the target receptor, as shown in **Table 2**. Among the docked compounds, derivative 2 (-10.3 kcal/mol) exhibited the most significant binding energy towards the targeted enzyme. This compound formed three hydrogen bonds with the amino acids TYR 382 and ASP 404. Additionally, van der Waals interactions were observed with the amino acids THR 383, ASP 384, GLY 523, and GLN 527. The roles of several key amino acids located in the active site of cholinesterase were studied and determined. Notable non-covalent interactions between the ligands were investigated. The active region targeted by molecules designed to inhibit cholinesterase was analyzed[32]. **Figure 2** illustrates the docking interactions of compound 2. Supplementary figure **S2-S23** shows both 2D and 3D interaction diagrams for all 10 synthesized compounds in comparison with the standard drug, donepezil.

Based on the docking results, ten derivatives were selected for synthesis using a conventional method. (E)-5-Styryl-1,3,4-oxadiazol-2-amine (A) was synthesized by reacting a mixture of semicarbazide and cinnamic acid in the presence of sulfuric acid. The reaction was heated at 65-75°C for about 22-24 hours. The completion of the reaction was monitored by TLC, using n-hexane:ethyl acetate as mobile phases in a 1:1 ratio, and visualized under UV light. Afterward, the mixture was cooled and basified by adding 50% NaOH with continuous stirring. The solid mass was collected by filtration. Next, compound A was reacted with different aromatic aldehydes in the presence of ethanol and NaOH, resulting in the corresponding N-(5-styryl-1,3,4-oxadiazol-2-yl)benzamide derivatives (1-5, and 51-55). All compounds and intermediates were purified by successive recrystallization from ethanol.

Table 2. Docking score of designed oxadiazole derivatives

Code	Binding affinity	Code	Binding affinity	Code	Binding affinity	Code	Binding affinity
1	-10.1	26	-6.5	51	-9.5	76	-8.1
2	-10.3	27	-8.2	52	-9.4	77	-8.1
3	-9.8	28	-8.6	53	-9.2	78	-8.5
4	-9.7	29	-7.2	54	-10.4	79	-8.3
5	-9.7	30	-7.4	55	-9.8	80	-8.1
6	-7.3	31	-7.4	56	-7.6	81	-8.0
7	-8.4	32	-6.0	57	-7.6	82	-8.1
8	-7.9	33	-8.9	58	-7.8	83	-9.2
9	-8.5	34	-8.1	59	-7.5	84	-9.0
10	-8.2	35	-8.9	60	-7.7	85	-9.1
11	-8.1	36	-8.8	61	-7.9	86	-8.9
12	-8.4	37	-8.5	62	-7.2	87	-8.8
13	-8.6	38	-8.2	63	-7.5	88	-8.6
14	-8.7	39	-8.4	64	-7.5	89	-8.7
15	-8.5	40	-8.3	65	-7.4	90	-8.6
16	-8.7	41	-7.1	66	-7.3	91	-8.3
17	-8.4	42	-7.6	67	-7.7	92	-8.1
18	-8.3	43	-7.2	68	-8.4	93	-8.5
19	-8.9	44	-7.1	69	-8.0	94	-9.1
20	-8.2	45	-7.3	70	-9.0	95	-8.4
21	-9.0	46	-7.3	71	-9.1	96	-8.1
22	-7.1	47	-7.4	72	-9.3	97	-8.7
23	-7.7	48	-7.4	73	-9.2	98	-8.7
24	-8.9	49	-7.6	74	-9.0	99	-8.5
25	-8.4	50	-7.8	75	-9.0	100	-8.8

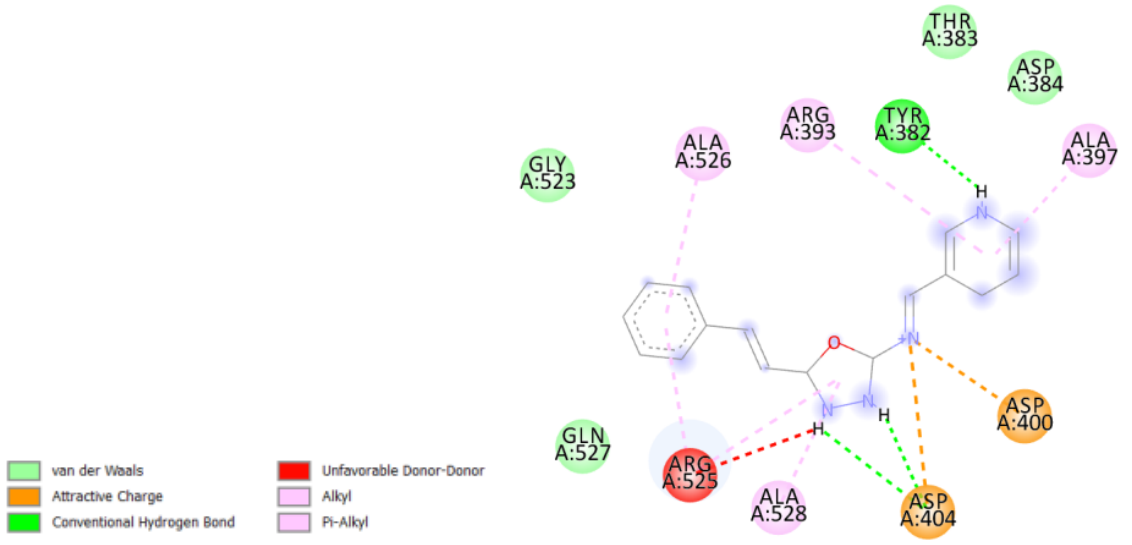

Figure 2. Fitting pose with interactions of compound 2 in the active site of 4EY6 in 2D view

The physical properties of all synthesized molecules are summarized in **Table 2**. The IR spectrum of the final synthesized compounds showed absorption peaks at 3350-3157 cm^{-1} for NH, 1489-1464 cm^{-1} for CH_2, 1379-1344 cm^{-1} for alkanes, and 800-700 cm^{-1} for aromatic rings were also present. These compounds exhibited appropriate peaks in their ^1H NMR spectra. The ^1H-NMR revealed a singlet signal in the range of 9.3-9.7 ppm for the secondary amine hydrogen, a singlet in the range of 8-8.5 ppm for the SP^2 hydrogen, and signals in the range of 7.5-8.5 ppm for the aromatic ring hydrogens. The ^{13}C-NMR showed signals in the range of 160-175 ppm for the C=O carbon, 150-160 ppm for the ethene carbon, and 120-145 ppm for the aromatic carbon. All the spectral data are given in supplementary figure **S24 - S63**. The assigned structures were confirmed by matching molecular ion peaks in the LC-MS. Short-term *in vitro* cytotoxicity tests using Alzheimer's cell lines and *in vitro* enzymatic assays using an appropriate assay kit were performed on all of the synthesized compounds[33].

In vitro evaluation of neuroprotective activity of synthesized compounds

The cell viability of SH-SY5Y cells was reduced to 53% when inoculated with BA, as determined by the absorbance of formazan crystals formed by the action of living cells. The viability percentage of standard and the synthesized compounds was checked by the concentration ranges from 5 - 80 µM concentration. The percentage of viability was calculated by standard protocol. The percentage viability of compound 2 was found to be 91.29%, and which was almost equal to that of the standard (92.35%), while the remaining compounds showed moderate to good neuroprotective activity. The optimum activity of compound 2 is due to the presence of favorable nitrogen containing heterocyclic bioisosters. **Table 3** represents the in-vitro neuroprotective activity of the synthesized compounds.

In vitro evaluation of acetyl cholinesterase inhibitory activity of synthesized compounds

The acetylcholinesterase inhibitory activity of the synthesized analogues was assessed using a modified Ellman's method and the results were communicated as IC_{50} values not set in stone by plotting the rate cell viability versus concentration of sample on a logarithmic chart and perusing the control[34]. The experiments were performed in triplicates, and then, the final IC50 values were calculated by taking an average of triplicate experimental results. Donepezil is used as reference drug for comparison. Enzyme activity for the control, standard, and synthesized compounds was determined under the same experimental conditions. The enzymatic activities of the solutions containing synthesized compounds and the standard were compared to those of the control to calculate the percentage inhibition of enzyme activity. The most significant cholinesterase catalytic domain inhibition was observed in compound 2 (IC_{50}=37.120±0.26 µM), which is nearly equivalent to the reference standard donepezil (IC_{50}=13.56±0.57 µM). The inhibitory effect of compound 2 is stronger than that of the other compounds examined, likely due to the presence of N-heterocyclic ring. The remaining compounds exhibited moderate to good acetylcholinesterase inhibitory activity. **Table 4** displays the results, and **Figure 3** provides a graphical representation of the enzyme inhibition activity of the synthesized compounds.

Table 3. Result for *In-vitro* neuroprotective activity of synthesized compounds

Compound code	Viability (%)
1	72.03
2	87.00
3	73.62
4	80.12
5	79.19
51	80.20
52	79.32
53	78.82
54	81.39
55	75.41
Donepezil	92.35

The research project focused on the design, synthesis, and evaluation of oxadiazoles as potential anti-Alzheimer's drugs has provided valuable insights into the field of Alzheimer's disease treatment. The careful design of novel oxadiazole derivatives and their effective synthesis have enabled a comprehensive assessment of their anti-Alzheimer efficacy. These newly synthesized compounds have shown great promise through a systematic evaluation

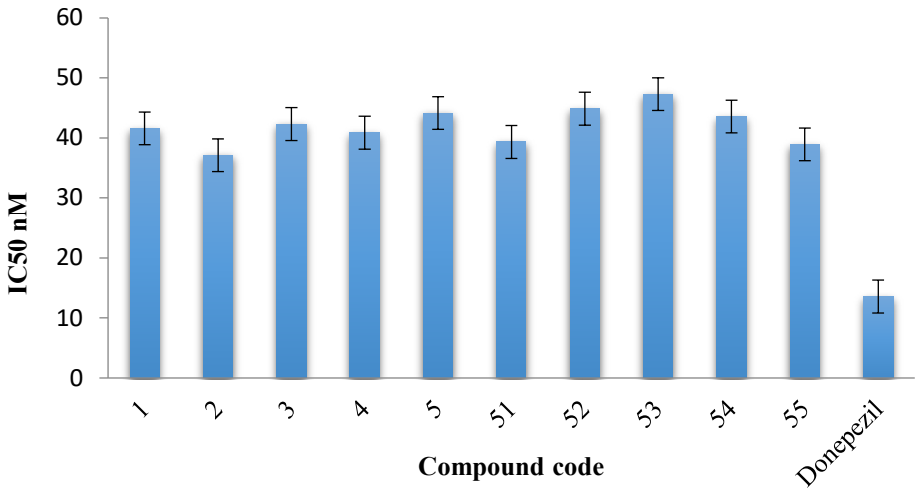

Figure 3. Graphical representation of enzyme inhibition activity of synthesized compounds

Table 4. Result for enzyme inhibition activity of synthesized compounds

Name of the compound	Enzyme inhibition activity (IC_{50} nM)
1	41.571±0.31
2	25.71±0.26
3	42.292±0.67
4	40.858±0.71
5	44.146±0.19
51	39.328±0.11
52	44.858±0.43
53	47.274±0.64
54	43.548±0.71
55	38.933±0.96
Donepezil	13.56±0.57

process, demonstrating their potential to modulate key biochemical pathways associated with Alzheimer's disease. To translate these promising molecules into clinical trials, collaboration with pharmaceutical companies and regulatory agencies will be crucial. Regulatory requirements and guidelines must be followed before proceeding to human trials. Long-Term Effects Given that Alzheimer's disease is a chronic condition, it is essential to evaluate the potential disease-modifying effects of these compounds over an extended period.

In this study, a series of substituted N-(5-((E)-styryl)-1,3,4-oxadiazol-2-yl)methanimine derivatives were designed, synthesized, and evaluated for their potential anti-Alzheimer activity. The molecular design was inspired by the structural versatility and pharmacological significance of the 1,3,4-oxadiazole core, which has been reported to exhibit AChE inhibitory and neuroprotective properties.

The synthesized compounds were characterized using FT-IR, NMR, and Mass spectrometry to confirm their structural integrity. Their AChE inhibitory potential was assessed through *in vitro* enzymatic assays, using Donepezil as a reference inhibitor. Molecular docking studies were performed against AChE (PDB ID: 4EY6) to elucidate the binding interactions and rationalize the observed biological activity. Further, neuroprotection assays were conducted using SH-SY5Y neuroblastoma cells, evaluating the compounds' ability to mitigate H_2O_2-induced oxidative stress and Aβ-induced cytotoxicity. Selected potent inhibitors were further subjected to ADME analysis to assess their drug-likeness and pharmacokinetic properties.

Molecular docking of 100 designed oxadiazole derivatives against acetylcholinesterase revealed promising binding affinities (−7.0 to −10.4 kcal/mol), with compound 2 (−10.3 kcal/mol) and compound 54 (−10.4 kcal/mol) showing the strongest interactions through hydrogen bonds with TYR382 and ASP404 and favorable van der Waals contacts. *In vitro* MTT assays on SH-SY5Y cells further confirmed the neuroprotective potential of these molecules, where compound 2 exhibited the highest viability (87.0%), comparable to the standard donepezil (92.3%), while compound 54, despite the best docking score, demonstrated only moderate activity (81.4%).

Overall, docking and biological results showed a weak correlation, highlighting that factors beyond binding affinity, such as cellular uptake and stability, influence neuroprotection. Compound 2 thus emerges as the most promising lead, combining strong target engagement with potent cell-based efficacy, warranting further enzymatic and pharmacokinetic evaluations.

The findings of this study indicate that the synthesized N-(5-((E)-styryl)-1,3,4-oxadiazol-2-yl) methanimine derivatives exhibit promising AChE inhibitory activity with potential neuroprotective effects. Molecular docking results revealed strong interactions within the CAS and PAS of AChE, suggesting a possible dual-binding inhibition mechanism. Among the tested compounds, Compoun 2 displayed the highest AChE inhibitory activity (IC_{50} = 37.120±0.26 μM μM), comparable to Donepezil. Additionally, the cytoprotective assays demonstrated that the selected derivatives could significantly attenuate oxidative stress-induced neuronal damage, highlighting their potential as multifunctional anti-Alzheimer agents overall, these study provides valuable insights into the SAR of oxadiazole-based AChE inhibitors and establishes a foundation for further optimization and preclinical investigations. Future studies will focus on *in vivo* evaluation and lead optimization to enhance selectivity, efficacy, and blood-brain barrier (BBB) permeability, paving the way for the development of novel therapeutic agents for Alzheimer's disease.

Disclosure of interest
Authors declare there is no conflict of interest.

Funding
No funding

Data availability
Data will be made available on request.

Supplementary data
The supplementary materials for this article comprise Figures S1 through S63.

References

1. **Hameed, H.A., Sankaranarayanan, M., Syazwani, A., Subhash, C., Mohammed, M.A., Taibi, B.H., Sonam, S., Mohammad, R., Fadhil, P., et al. (2022).** Novel thiophene chalcones-coumarin as acetylcholinesterase inhibitors: Design, synthesis, biological evaluation, molecular docking, ADMET prediction and molecular dynamics simulation. Bioorganic Chemistry. 119: 105572.
2. **Elumalai, K., Shanmugam, A., Devaraji, M., Srinivasan, S. (2024).** Synthesis and molecular docking of pyrimidine derivatives as antibacterial agents. Carbon Resources Conversion. 7(3): 100222.
3. **Piplani, P., Jain, A., Devi, D., Anjali, Sharma, A., Silakari, P. (2018).** Design, synthesis and pharmacological evaluation of some novel indanone derivatives as acetylcholinesterase inhibitors for the management of cognitive dysfunction. Bioorganic & Medicinal Chemistry. 26(1): 215-224.
4. **Helmi, M.A., Hameed, H.A., Mustapha, S., Muhammad Asraf, A.Z., et al. (2024).** Benzyloxychalcone hybrids as prospective acetylcholinesterase inhibitors against Alzheimer's disease: Rational design, synthesis, *in silico* ADMET prediction, QSAR, molecular docking, DFT, and molecular dynamic simulation studies. ACS Omega. 30(9): 6115-6130.
5. **Kontaxi, C., Piccardo, P., Gill, A.C. (2017).** Lysine-directed post-translational modifications of tau protein in Alzheimer's disease and related tauopathies. Frontiers in Molecular Biosciences. 4: 56.
6. **Smith, M.A., Rottkamp, C.A., Nunomura, A., Raina, A.K., Perry, G. (2000).** Oxidative stress in Alzheimer's disease. Biochimica et Biophysica Acta - Molecular Basis of Disease. 1502: 139-144.
7. **Namgoong, J.H., Bertoni, C. (2016).** Clinical potential of ataluren in the treatment of Duchenne muscular dystrophy. Degenerative Neurological and Neuromuscular Disease, 6: 37-48.
8. **Kim, A.C., Lim, S., Kim, Y.K. (2018).** Metal ion effects on Aβ and tau aggregation. International Journal of Molecular Sciences. 19: 128.
9. **Yu, W., Cheng, L.P., Pang, W., Guo, L.L. (2022).** Design, synthesis and biological evaluation of novel 1,3,4-oxadiazole derivatives as potent neuraminidase inhibitors. Bioorganic & Medicinal Chemistry. 57: 116647.
10. **Luo, L., Ou, Y., Zhang, Q., Gan, X. (2023).** Discovery of 1,2,4-oxadiazole derivatives containing haloalkyl as potential acetylcholine receptor nematicides. International Journal of Molecular Sciences. 24(6): 5773.
11. **Nazari, M., Rezaee, E., Hariri, R., Akbarzadeh, T., Tabatabai, S.A. (2021).** Novel 1,2,4-oxadiazole derivatives as selective butyrylcholinesterase inhibitors: Design, synthesis and biological evaluation. EXCLI Journal, 20: 907.
12. **Anwar, S., Rehman, W., Hussain, R., Khan, S., Alanazi, M.M., Alsaif, N.A., Khan, Y., Iqbal, S., Naz, A., Hashmi, M.A. (2023).** Investigation of novel benzoxazole-oxadiazole derivatives as effective anti-

Alzheimer's agents: *In vitro* and *in silico* approaches. Pharmaceuticals, 16(7): 909.
13. **Henstridge, C.M., Pickett, E., Spires-Jones, T.L. (2016).** Synaptic pathology: A shared mechanism in neurological disease. Ageing Research Reviews. 28: 72-84.
14. **Saira, N., Ahmed, T., Aqeel, I., Saquib, J., Shamool, F., Parham, T., Jamshed, I., Mussarat, T., Muhammad, N., Zahid, S. (2023).** Therapeutic potential of 1,3,4-oxadiazoles as potential lead compounds for the treatment of Alzheimer's disease. RSC Advances. 13: 17526.
15. **Rehman, A.U., Nafeesa, K., Abbasi, M.A. (2018).** Synthesis of new heterocyclic 3-piperidinyl-1,3,4-oxadiazole derivatives as potential drug candidate for the treatment of Alzheimer's disease. Cogent Chemistry. 4(1): 1472197.
16. **Jayaraj, S., Hemalatha, K. (2024).** Design, synthesis, and anticancer evaluation of novel N-[5-(1,3,4,5-tetrahydroxycyclohexyl)-1,3,4-thiadiazole-2-yl] benzamide analogues through integrated computational and experimental approaches. Future Journal of Pharmaceutical Sciences. 10: 149.
17. **Renukadevi, J., Karthikha, V.S., Sam Helinto, J., Prena, D., Arockiya Rabin, A. (2024).** Molecular dynamic simulation studies of Hemidesmus indicus-derived oleanen-3-yl acetate in STAT3-based tumor signaling. Journal of Applied Pharmaceutical Research. 12(5): 124-132.
18. **Kaur, M., Singh, S., Kaur, M. (2018).** Synthesis, spectral study and biological activity of some 2,5-disubstituted 1,3,4-oxadiazole. European Journal of Pharmaceutical and Medical Research. 5(9): 277-282.
19. **Ahsan, M.J. (2018).** Synthesis and cytotoxicity evaluation of [(2,4-dichlorophenoxy)methyl]-5-aryl-1,3,4-oxadiazole/4H-1,2,4-triazole analogues. Turkish Journal of Chemistry. 42(5): 1334-1343.
20. **Glomb, T., Swiatek, P. (2021).** Antimicrobial activity of 1,3,4-oxadiazole derivatives. International Journal of Molecular Sciences. 22: 6979.
21. **Agarwal, M., Singh, V., Sharma, S.K., Sharma, P., Ansari, M.Y., Jadav, S.S., Ahsan, M.J. (2019).** Design and synthesis of new 2,5-disubstituted-1,3,4-oxadiazole analogues as anticancer agents. Medicinal Chemistry Research. 25(10): 2289-2303.
22. **Singh, P., Jangra, P.K. (2010).** Oxadiazoles: A novel class of anti-convulsant agents. Pelagia Research Library. 1(3): 118-123.
23. **Bala, S., Kamboj, S., Kumar, A. (2010).** Heterocyclic 1,3,4-oxadiazole compounds with diverse biological activities: A comprehensive review. Journal of Pharmaceutical Research. 3(12): 2993-2997.
24. **James, N.D., Growcott, J.W. (2009).** Zibotentan endothelin ETA receptor antagonist oncolytic. Drugs of the Future. 34(8): 624-633.
25. **Farida, B., Muhammad, Y., Sajid, I., Nazif, U., Anwar, H., Momin, K., Asaad, K., Alanood, S.A., Ashraf, N.A. (2019).** Inhibition of acetylcholinesterase with novel 1,3,4-oxadiazole derivatives: A kinetic, *in silico*, and *in vitro* approach. ACS Omega. 8(49): 46829.
26. **Nazir, M., Abbasi, M.A., Aziz-Ur-Rehman, Siddiqui, S.Z., Raza, H., Hassan, M., Ali Shah, S.A., Shahid, M., Seo, S.Y. (2018).** Novel indole-based hybrid oxadiazole scaffolds with N-(substituted-phenyl)butanamides: Synthesis, Lineweaver-Burk plot evaluation and binding analysis of potent urease inhibitors. RSC Advances. 8(46): 25920-25931.
27. **Abbasi, M.A., Hassan, M., Aziz-Ur-Rehman, Siddiqui, S.Z., Raza, H., Shah, S.A.A., Seo, S.Y. (2018).** Synthesis, *in vitro* and *in silico* studies of novel potent urease inhibitors: N-[4-({5-[(3-un/substituted-anilino-3-oxopropyl)sulfanyl]-1,3,4-oxadiazol-2-yl} methyl)-1,3-thiazol-2-yl]benzamides. Bioorganic & Medicinal Chemistry. 26(13): 3791-3804.
28. **Jones, A.M., Helm, J.M. (2009).** Emerging treatments in cystic fibrosis. Drugs. 69: 1903-1910.
29. **Anwar, S., Rehman, W., Hussain, R., Khan, S., Alanazi, M.M., Alsaif, N.A., Khan, Y., Iqbal, S., Naz, A., Hashmi, M.A. (2023).** Investigation of novel benzoxazole-oxadiazole derivatives as effective anti-Alzheimer's agents: *In vitro* and *in silico* approaches. Pharmaceuticals. 16(7): 909.
30. **Ducharme, Y., Blouin, M., Brideau, C., Châteauneuf, A., Gareau, Y., Grimm, E.L., Juteau, H., Laliberte, S., MacKay, B., Masse, F., Ouellet, M. (2010).** The discovery of setileuton, a potent and selective 5-lipoxygenase inhibitor. ACS Medicinal Chemistry Letters. 1(4): 170-174.
31. **de Oliveira, C.S., Lira, B., Barbosa Filho, J.M., Lorenzo, J.G., de Athayde-Filho, P.F. (2012).** Synthetic approaches and pharmacological activity of 1,3,4-oxadiazoles: A review of the literature from 2000-2012. Molecules. 17(9): 10192-10231.
32. **Kaviarasan, L., Gowramma, B., Kalirajan, R., Mevithra, M., Chandralekha, S. (2020).** Molecular docking studies and synthesis of a new class of chroman-4-one fused 1,3,4-thiadiazole derivatives and evaluation for their anticancer potential. Journal of the Iranian Chemical Society. 17(8): 2083-2094.
33. **Swathi, K., Gowramma, B., Manal, M. (2019).** Synthesis, *in silico* and *in vivo* evaluation of novel 1,3,4-thiadiazole analogues as novel anticancer agents. Letters in Drug Design & Discovery. 16: 1-11.
34. **Ellman, G.L., Courtney, K.D., Andres, V., Featherstone, R.M. (1961).** A new and rapid colorimetric determination of acetylcholinesterase activity. Biochemical Pharmacology. 7(2): 88-95.